JURNAL MATEMATIKA, STATISTIKA DAN KOMPUTASI e–ISSN: 2614–8811
Published by Departement of Mathematics, Hasanuddin University, Indonesia
https://journal.unhas.ac.id/index.php/jmsk/index

Vol. 22, No. 3, May 2026, pp. 655-670
DOI: 10.20956/j.v22i3.49930

Unveiling Eco-Epidemiological Risk Assessment through Bayesian Spatio-Temporal SPDE-INLA Approach

Mukhsar[1*], Ida Usman[2], Asrul Sani[3], La Gubu[4], Muzuni[5], Ruslan Majid[6], I Putu Sudayasa[7], Fahmiati[8]

[1]Department of Statistics Faculty of Mathematics and Natural Sciences Halu Oleo University, Kendari-Indonesia
[2]Department of Physics Faculty of Mathematics and Natural Sciences Halu Oleo University, Kendari-Indonesia
[3,4]Department of Mathematics Faculty of Mathematics and Natural Sciences Halu Oleo University, Kendari-Indonesia
[5]Department of Biology Faculty of Mathematics and Natural Sciences Halu Oleo University, Kendari-Indonesia
[6]Public Health Department Faculty of Public health Halu Oleo University, Kendari-Indonesia
[7]Medical Department Faculty of Medicine Halu Oleo University, Kendari-Indonesia
[8]Department of Chemistry Faculty of Mathematics and Natural Sciences Halu Oleo University, Kendari-Indonesia
***Email:** [1]email: mukhsar.mtmk@uho.ac.id, [2]ida.usman@uho.ac.id, [3]saniasrul2001@yahoo.com, [4]la.gubu@uho.ac.id, [5]muzuni_fmipa@uho.ac.id, [6]ruslan.madjij@uho.ac.id, [7]dr.putusudaysa@uho.ac.id, [8]fahmiati@uho.ac.id*
**Corresponding author*
Received: 15 December 2026, revised: 8 April 2026, accepted: 13 April 2026

Abstract

Dengue hemorrhagic fever (DHF) remains a major public health burden in tropical areas. The DHF driven by nonlinear interactions, vector dynamics, and population density. Characterizing spatio-temporal risk heterogeneity is critical to targeted intervention. We analyzed dengue risk in Kendari using a Bayesian Stochastic Partial Differential Equation (SPDE) via Integrated Nested Laplace Approximation (INLA). DHF monthly data from 2022–2024 were integrated with geospatial information to estimate relative risk and spatial risk contours. Model performance was compared with Generalized Linear Models (GLM), Intrinsic Conditional Autoregressive (ICAR), and second order Random Walk (RW2). Kendari Barat and Kendari districts emerged as primary hotspots, while Kadia, Mandonga, Baruga, Kambu, and Wua-Wua were high-risk districts. Abeli, Poasia, and Puuwatu districts exhibited moderate risk. Lalodati, Soropia, and Sampara districts showed lower risk. Risk contours revealed clusters concentrated in the urban core and along major corridors, highlighting the influence of settlement density and spatial connectivity. The SPDE–INLA model outperformed GLM, ICAR, and RW2 in capturing spatial structure and improving

predictive accuracy. High resolution risk estimates supported specific district including intensified source reduction before and during peak rainfall, selective fogging, larval control, community education, microclimate monitoring, and early case screening in high-risk areas.
Keywords: Bayesian, DHF, INLA, Relative Risk, SPDE.

1. INTRODUCTION AND PRELIMINARIES

Kendari City, the administrative and economic hub of Southeast Sulawesi Province, has undergone rapid urbanization over the past two decades, resulting in substantial environmental restructuring. Accelerated population growth, increasing urban density, widespread land-use conversion, and intensive infrastructure development have collectively reshaped the local ecological system [10]. These transformations have significantly influenced the spatial distribution and habitat suitability of *Aedes aegypti*, the primary vector of dengue hemorrhagic fever (DHF) [1,6] . The DHF incidence in Kendari City exhibits pronounced spatial heterogeneity across districts, reflecting localized variations in environmental exposure, human vector interactions, and socio-demographic conditions. Such fine scale eco epidemiological variability poses major challenges for conventional surveillance and intervention frameworks [9,14], which often rely on spatially aggregated indicators and static risk assumptions [13]. Consequently, there is a critical need for flexible spatially explicit modeling approaches capable of capturing both structured and unstructured heterogeneity in disease risk, thereby providing a more robust for targeted dengue prevention and control [2,8].

This spatial complexity necessitates a modeling framework capable of adaptively characterizing dynamic risk patterns [18]. Nevertheless, the underlying ecological and epidemiological interactions are often insufficiently represented by conventional statistical techniques, including Generalized Linear Models (GLM), kriging, and CAR/SAR specifications [19]. A key limitation of these approaches lies in their formulation over discrete spatial units, which restricts their ability to adequately capture disease risk processes evolving continuously across geographic space [4]. In contrast, the Bayesian Stochastic Partial Differential Equation (SPDE) approach offers a principled framework for approximating continuous spatial fields through a Gaussian Markov Random Field (GMRF) representation defined on a triangulated mesh [5,11]. When integrated with the Integrated Nested Laplace Approximation (INLA), this framework enables the construction of highly flexible spatio-temporal models while maintaining computational efficiency and numerical stability, thereby facilitating scalable inference for complex disease mapping applications [12].

The SPDE-INLA framework enables the integration of high-resolution environmental predictors, including rainfall, air temperature, relative humidity, and the Normalized Difference Vegetation Index (NDVI) to flexibly characterize both linear and nonlinear associations between environmental variability and DHF risk [15]. Rainfall facilitates the creation of larval habitats, temperature modulates viral replication and vector development rates, while relative humidity influences adult mosquito longevity. Within this spatio-temporal modeling framework, the SPDE-INLA yields posterior risk surfaces and exceedance probability maps that provide a quantitative basis for prioritizing areas in informed risk vector control planning [16]. This approach supports the detection of latent risk clusters, reconstruction of seasonal transmission dynamics, and continuous representation of disease risk independent of administrative boundaries.

Beyond enhancing dengue early warning capacity in Kendari City, the proposed framework contributes methodologically to eco-epidemiological research in Indonesia by demonstrating the applicability of Bayesian SPDE-INLA for environmentally driven disease modeling in tropical urban settings [17]. This study aims to develop a Bayesian SPDE-INLA-based spatio-temporal

dengue model for Kendari City to identify transmission hotspots and seasonal patterns, thereby supporting evidence-based vector control strategies. The novelty of this work resides in the integration of Bayesian SPDE-INLA with high-resolution environmental predictors to model dengue risk as a continuous spatio-temporal process at the district level, enabling more precise hotspot detection and seasonal characterization than conventional discrete spatial approaches in the Indonesian tropical urban context.

2. METHODS

2.1. RESEARCH LOCATION

This research was carried out in Kendari City, the capital of Southeast Sulawesi Province, Indonesia, which comprises of 13 districts exhibiting pronounced geomorphological and environmental heterogeneity. Spatially, the central to eastern parts of the city is dominated by the coastal zone of Kendari Bay, whereas the western and southern regions are characterized by lowland areas that gradually transition into hilly terrain. Elevation across the city ranges from approximately 0 to 200 m above sea level, with slope gradients varying from gentle to steep, particularly in the Mataiwoi, Baruga, and Kambu districts. Such topographic diversity gives rise to localized microclimatic conditions, shapes surface runoff dynamics, and influences the spatial distribution of potential *Aedes aegypti* breeding habitats, primarily through the formation of temporary water accumulations and areas with inadequate drainage.

Kendari City lies within a humid tropical climate regime, with annual precipitation ranging from approximately 1.800 to 2.500 mm, mean air temperatures of 26–28°C, and relative humidity levels between 75% and 90%. Seasonal variability is primarily governed by the regional monsoon system and large-scale climate oscillations, notably the El Niño Southern Oscillation (ENSO) and the Indian Ocean Dipole (IOD), which episodically modulate rainfall intensity, atmospheric moisture, and the duration of wet and dry periods. These climatic drivers exert a direct influence on dengue vector ecology by regulating larval development rates, adult mosquito survival, and biting frequency. These processes shape the spatio-temporal patterns of dengue transmission across Kendari City.

Kendari City also is undergoing rapid urbanization, manifested through the expansion of built-up areas, shifts in land cover composition, reduction of green spaces, and the emergence of microhabitats favorable to dengue transmission. These landscape transformations increase environmental heterogeneity, which is reflected in the spatial variability of dengue incidence across districts. Dengue fever in Kendari City displays pronounced interannual fluctuations and uneven spatial patterns, particularly in densely populated areas characterized by intensive socioeconomic activities and complex urban drainage networks. Conversely, coastal districts tend to be influenced by elevated humidity, sea breeze circulation, and tidally driven surface water dynamics, which further modulate local transmission conditions.

Kendari City was selected as the study area based on several compelling scientific considerations. The city exhibits pronounced epidemiological heterogeneity across districts and seasons, providing a suitable setting for investigating spatio-temporal variability in dengue risk. In addition, Kendari City encompasses diverse environmental conditions that support the integration of multiple eco environmental drivers within the modeling framework. Ongoing rapid spatial transformations further enhance its relevance as a representative urban landscape for developing and evaluating eco epidemiological risk models formulated over continuous spatial domains.

2.2. RESEARCH DESIGN

The analysis was conducted within a spatio-temporal modeling framework using monthly data spanning the period 2022–2024. This temporal resolution enables finer characterization of risk dynamics while simultaneously capturing spatial variability that is often obscured by conventionally aggregated data [20]. Accordingly, the proposed model not only quantifies differences in dengue incidence across districts but also represents risk evolution as a continuous process in both space and time [22].

The model specification comprises three principal components. First, an observation model defines the probabilistic distribution of reported dengue cases [21]. Second, a latent process component incorporates environmental covariates and random effects to account for structured and unstructured heterogeneity. Third, a continuous spatial field is constructed using the SPDE-INLA formulation and coupled with a temporal dependence structure to capture correlations between successive time periods [6,23]. Together, these components provide a coherent and flexible framework for elucidating complex dengue risk patterns and their underlying eco-epidemiological mechanisms.

2.3 DATA

Monthly dengue case counts at the district level for the period 2022–2024 were obtained from the Kendari City Health Office. Predictor variables comprised climate related parameters sourced from the Indonesian Agency for Meteorology, Climatology, and Geophysics (BMKG) and the ERA5-Land dataset, including rainfall (mm), surface air temperature (°C), and relative humidity (%).

ERA5-Land is a high-resolution global climate reanalysis product that has been widely applied in environmental climatology and epidemiological studies [3]. Environmental conditions are known to strongly influence *Aedes* mosquito population dynamics and dengue transmission risk [24]. Accordingly, incorporating climate covariates into the spatio-temporal modeling framework enhances predictive performance and supports a more comprehensive characterization of dengue epidemiological in Kendari City.

2.4 MODEL FORMULATION

DHF case counts represent discrete observations and frequently display overdispersion, accordingly, the likelihood was specified using a negative binomial distribution to account for variability exceeding that expected under a Poisson assumption.

$$Y(s,t) \sim NB(\lambda(s,t), \theta),$$

and predictor:

$$\log \lambda(s,t) = \beta_0 + \beta X(s,t) + u_s(s) + u_t(t) + \omega_{st}(s,t)$$

with

$X(s,t)$ as environmental predictor at location s time t,
$u_s(s)$ as spatial effects of SPDE,
$u_t(t)$ as temporal effects RW2,
$\omega_{st}(s,t)$ as spatial-temporal interaction.

Within the SPDE framework, spatial dependence is represented through a Matérn-type SPDE of the form $(\kappa^2 - \Delta)^{\alpha/2} u_s(s) = W(s)$, where κ controls the spatial range, α governs field smoothness, and $W(s)$ denotes Gaussian white noise [7,24]. This formulation yields a Gaussian Markov Random Field (GMRF) approximation characterized by a sparse precision matrix $Q(\kappa, \tau)$,

constructed over a triangulated mesh and regularized using penalized complexity Matérn priors to ensure model parsimony and stability.

The temporal component was specified using a RW2, selected based on WAIC and DIC criteria [17]. The resulting spatio-temporal interaction was expressed as $\omega_{st}(s,t) = u_s(s)\, u_t(t)$, allowing spatial patterns to evolve smoothly over time. This modeling strategy has demonstrated strong performance for environmentally driven diseases, including dengue in tropical regions, particularly when combined with high resolution climate predictors [24].

Posterior risk intensity surfaces were summarized by the posterior mean $\hat{\lambda}(s,t) = E[\lambda(s,t) \mid \text{data}]$, producing continuous dengue risk maps for each time period. Uncertainty was quantified using exceedance probability maps, defined as $P(\lambda(s,t) > c \mid \text{data})$, where locations with probabilities exceeding 0.8 were designated as priority areas for intervention [23].

3. RESULTS AND DISCUSSION

The distribution of DHF cases during the study period exhibited a markedly right skewed (Figure 3.1), with most districts reporting relatively low case counts, while a limited number experienced pronounced surges during specific months [2,7].

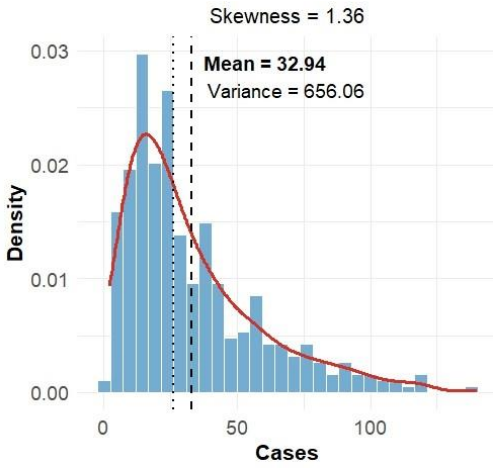

Figure 3.1. Monthly distribution of DHF cases in Kendari City during 2022–2024

These indicate the presence of localized environmental conditions that are highly favorable for *Aedes* vector proliferation and dengue transmission [1]. The observed variance exceeding the mean provides clear evidence of overdispersion, rendering conventional Poisson models inadequate for capturing the underlying data structure [6]. Moreover, the pronounced spatial heterogeneity across districts suggests that case dynamics cannot be adequately explained by simple linear models without accounting for spatial random effects [4]. These characteristics provide methodological justification for adopting a Bayesian Negative Binomial specification [16,23].

Time series analysis further reveals that dengue incidence typically peaks one to two months following periods of maximum rainfall (Figure 3.2). This temporal lag is consistent with the biological dynamics of *Aedes aegypti*, encompassing the egg-larva-pupa developmental stages and the extrinsic incubation period of the dengue virus within the mosquito vector [12].

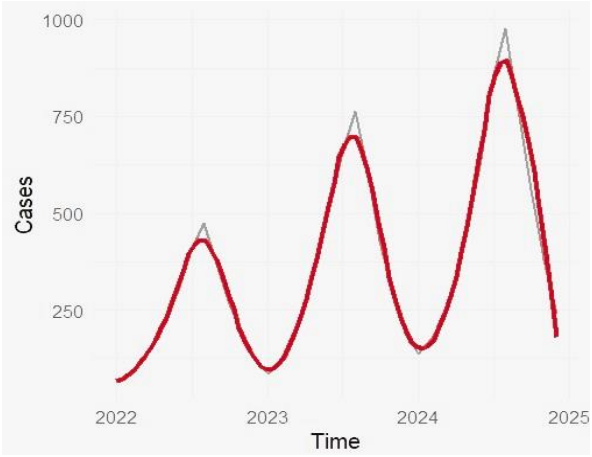

Figure 3.2. Monthly trends and seasonal of DHF cases during 2022–2024

An additive time series decomposition of monthly DHF case counts in Kendari City for the 2022–2024 period was performed to separate the observed series into trend, seasonal, and residual components (Figure 3.3). The observation component exhibits recurring annual fluctuations, with increasingly pronounced peaks toward the latter part of the study period. The trend component indicates a gradual upward trajectory, suggesting the presence of long term dengue risk dynamics beyond purely seasonal variation.

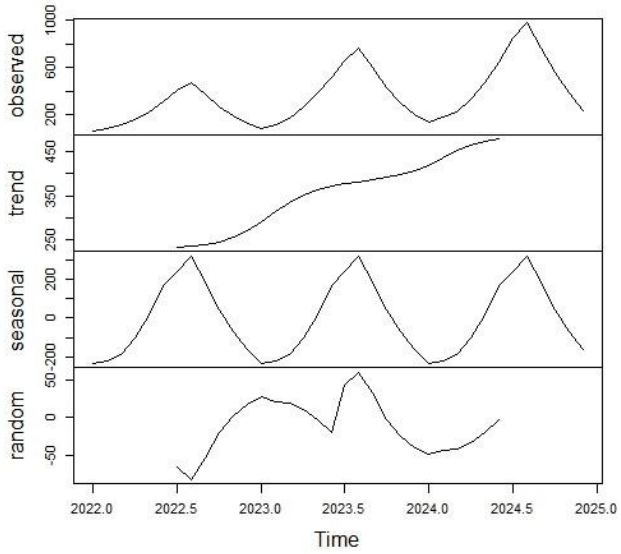

Figure 3.3. Time series decomposition

Seasonal patterns remain consistent across years, reflecting the strong influence of climatic drivers, particularly rainfall, temperature, and relative humidity on dengue transmission dynamics [14]. In contrast, the residual component is comparatively small and displays random fluctuations, indicating that most temporal variability is adequately captured by the combined trend and seasonal structures. Collectively, these findings demonstrate that dengue dynamics in Kendari City are

characterized by strong seasonality accompanied by an increasing trend. This behavior further supports the adoption of a Bayesian spatio-temporal modeling framework capable of simultaneously accommodating temporal dependence and environmental drivers [9].

The observed lagged response pattern (Figure 3.4) further confirms that the effects of environmental drivers on dengue incidence are not instantaneous, highlighting the necessity of incorporating lag structures into the modeling framework to obtain reliable risk estimates [22]. Spatial patterns reveal implicit associations between elevated case counts and residential density, population mobility, and urban drainage conditions [18]. These findings reinforce the understanding that dengue risk is shaped not only by ecological determinants but also by social structure and urban spatial configuration [2,7].

The adoption of a continuous domain spatial modeling approach via SPDE-INLA is particularly well suited for capturing unobserved spatial heterogeneity and complex transmission landscapes that cannot be adequately represented by discrete area models [6].

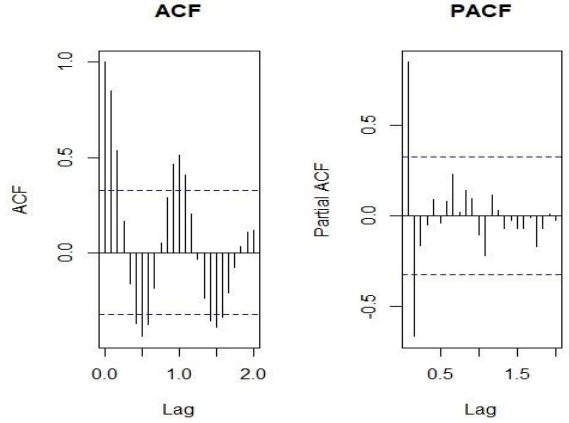

Figure 3.4. Autocorrelation

A Moran's I value of 0.41 ($p < 0.01$) (see Figure 3.5) indicates statistically significant spatial clustering of dengue hemorrhagic fever (DHF) cases. Areas with elevated incidence are likely to increase risk in neighboring districts through spatial spillover mechanisms, driven by vector dispersal, shared habitat characteristics, and inter-area human mobility [16]. Climatic conditions in Kendari City characterized by monthly rainfall ranging from 92 to 482 mm, temperatures between 25.3 and 28.9 °C, and relative humidity levels of 68–89% provide a favorable environment for the survival and activity of *Aedes aegypti*.

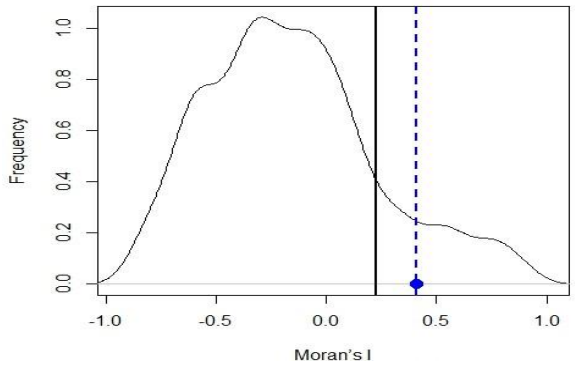

Figure 3.5. Monte Carlo simulation of Moran's Index

The precision matrix Q constitutes a central component of the GMRF representation arising from the SPDE approximation, enabling highly efficient posterior computation within the INLA framework [12]. The procedure begins with the construction of a spatial triangulation mesh, where the latent spatial field $u_s(s)$ is approximated using linear finite element basis functions [5].

$$u_s(s) \approx \sum_{i=1}^{n} u_i \, \phi_i(s),$$

with $\phi_i(s)$ denoting the linear basis function associated with the i-th mesh node. This formulation transforms the continuous spatial domain into a discrete dependency structure defined over mesh nodes.

Within the finite element framework, two fundamental matrices characterize the mesh geometry and the differential operator of the SPDE. The mass matrix M, representing inner products of basis functions, is given by

$$M_{ij} = \int_{\Omega} \phi_i(s) \, \phi_j(s) \, ds,$$

while the stiffness matrix K, encoding the Laplacian operator (Δ), is defined as

$$K_{ij} = \int_{\Omega} \nabla \phi_i(s) \cdot \nabla \phi_j(s) \, ds.$$

The combination of these matrices forms the basis of the Matérn operator in the SPDE formulation. The resulting precision matrix Q exhibits a sparse structure, such that each node interacts only with its immediate neighbors within the same triangular elements. Non zero entries in Q therefore occur exclusively between geographically adjacent nodes, reflecting localized spatial dependence. Diagonal elements of Q quantify uncertainty in risk at a given location, whereas negative off diagonal elements indicate that changes in risk at one node directly influence its nearest neighbors. The precision matrix governs how dengue risk is distributed, propagated, and spatially correlated across the continuous domain of Kendari City, providing a mechanistic representation of local dependence and spatial diffusion within the SPDE-INLA framework.

The spatial mesh constitutes a core component of the SPDE framework, as it defines the numerical representation of the study domain. In this study, the mesh was constructed using administrative boundaries as the inner domain and extended by an outer buffer of approximately 5 km to mitigate boundary effects. An adaptive triangulation strategy was adopted, with finer elements in densely populated areas such as Kendari Barat, Kadia, and Poasia districts to enhance predictive resolution, and coarser elements in coastal and vegetated regions including Abeli and Nambo districts. Mesh density was aligned with local morphology and geomorphological contours, yielding a spatial representation that realistically reflects the underlying Matérn process. The SPDE operator $(\kappa^2 - \Delta)^{\alpha/2} u_s(s) = W(s)$ is governed by key parameters, where κ controls the spatial scale (inverse range), α determines field smoothness, and $W(s)$ denotes Gaussian white noise. Within the Bayesian SPDE-INLA framework, spatial dependence is characterized through a Matérn predictors parameterized by κ and ν. Larger values of κ induce more localized spatial structure, producing sharper risk contrasts between neighboring areas, whereas smaller κ values enhance long-range correlation, resulting in broader hotspots and smoother risk gradients.

Kendari district exhibited the strongest spatial effect, acting as an epicenter of dengue transmission, likely driven by high population density, compact residential patterns, intense mobility, and limited green space [17]. Spatio-temporal effects peaked during December–February

(see Figure 3.2), consistent with dengue seasonality in humid tropical climates. Kendari Barat district showed persistently elevated risk throughout the year, forming a strong cluster with Kendari district, attributable to concentrated economic activity and dense settlement. Temporal effects intensified during the rainy season and persisted for several months, reflecting environmentally induced lag associated with the *Aedes* life cycle.

Mandonga district exhibited moderate to high risk, with mixed commercial residential land use and population mobility emerging as dominant drivers, consistent with increased human vector contact. Peak risk occurred early in the year but declined more rapidly than in Kendari Barat district. Baruga district characterized by rapid land cover change, displayed unstable risk patterns with localized hotspots, showing high sensitivity to moderate rainfall and highlighting the influence of landscape transformation on *Aedes* habitats. Kambu districts experienced moderate risk during February–April, in line with the typical 2–6 weeks lag between rainfall and dengue incidence.

Poasia district demonstrated elevated risk and spatial clustering with Kambu and Abeli districts, with heightened sensitivity to rainfall reflecting microenvironmental heterogeneity in newly urbanized areas. Abeli district, a semi-urban coastal district, exhibited moderate risk influenced by high humidity and seasonal surface water accumulation, consistent with dengue dynamics in tropical coastal settings. Nambo district, a sparsely populated coastal area, recorded the lowest risk, potentially due to sea breeze circulation reducing microscale humidity and constraining *Aedes* development. Kadia district showed moderate to high risk associated with population mobility and drainage related water pooling, with spatio-temporal peaks observed during February–March. Wua-Wua district displayed relatively stable moderate risk, with sensitivity to temperature and local vegetation affecting microhabitat humidity. Finally, Puwatu district, located in hilly terrain (50–200 m above sea level), exhibited negative spatial effects or comparatively low risk, consistent with evidence that increasing elevation limits *Aedes* survival. A comprehensive summary of dengue distribution across Kendari City is provided in Table 3.1.

Table 3.1. Summary of district geographic characteristics and dengue risk zones in Kendari City

Risk Zone	Districts	Characteristics
High Risk	Kendari, Kendari Barat, Mandonga, Poasia	Dense urban settlements, rapid infrastructure development, and complex drainage systems
Moderate Risk	Baruga, Kambu, Abeli, Kadia, Wua-Wua	Expanding residential areas with strong interactions between urbanization and environmental conditions
Low Risk	Nambo, Puwatu	Open coastal environments and higher-elevation terrain

Spatial effects were estimated through the latent field $u_s(s)$, modeled as a GMRF using the SPDE discretization approach. The estimated spatial range was $\rho \approx 11.5$ km. Given that the geographic extent of Kendari City is approximately 20 km, this result indicates that spatial dependence spans nearly the entire urban area. The posterior variance $\sigma^2 \approx 0.42$ suggests substantial spatial heterogeneity, consistent with documented microenvironmental variability in dense urban settings. Prominent hotspots were identified in Kambu, Anduonohu, and Wua-Wua districts. Coastal areas such as Abeli district exhibited negative spatial effects, reflecting comparatively lower risk associated with microclimatic conditions less favorable to vector persistence.

Temporal effects $u_t(t)$ were modeled using a RW2, a standard formulation for capturing seasonal structure and long-term trends. Posterior estimates reveal a gradual increasing trend over the 2022–2024 period, with consistent seasonal peaks occurring between December to March, in line with the wet monsoon and established dengue seasonality across Southeast Asia. Enhanced temporal variability observed in 2023 is plausibly linked to ENSO/La Niña-related climate anomalies, which intensified humidity levels and surface water accumulation.

The spatio-temporal interaction component $\omega_{st}(s,t)$ captured localized dynamics not explained by purely spatial or temporal terms, including pronounced case increases in Kambu and Anduonohu districts during early 2023. Incorporating this interaction substantially improved model performance, yielding a reduction in WAIC of approximately $\Delta\text{WAIC} \approx -63$. Model performance was further assessed by comparing the SPDE-INLA specification against three baseline models a Poisson GLM, a discrete spatial CAR model, and a temporal RW2 model using WAIC and DIC criteria, as summarized in Algorithm 3.1.

Algorithm 3.1

Input:

- DHF monthly data
  dhf $= \{(k_s, t_t, y_{st})\}$, k_s district s, t_t time t, and y_{st} is DHF cases
- Environmental data per district
  $$\text{env} = \{(k_s, t_t, x_{st})\}$$
- District shapefile of Kendari

Data Pra-Processing

- Convert time index to numeric variable:
  $$t_j \leftarrow \text{as.numeric(as.factor(time))}$$
- Data aggregate
  $$y_{st} = \sum y_{st}$$
- Merge the data into a district shapefile.
- Transform the coordinate system to a metric CRS (UTM).
- Assign the district numeric index.
  $$sd_s = 1,2, \ldots, n$$

GLM Poisson

- Parameter estimation
  $$y_{st} \sim \text{Poisson}(\lambda_{st}), \log(\lambda_{st}) = \beta_0$$
- Extract the posterior mean
  $$\hat{y}^{GLM}$$

CAR (ICAR)

- Queen contiguity adjacency matrix.
- Adjacency graph.
  $$\log(\lambda_{st}) = \beta_0 + u_s, u_s \sim ICAR$$
- Extract:

$$\hat{y}^{CAR}$$

RW2 + ICAR

- Add temporal effect RW2:

$$\log(\lambda_{st}) = \beta_0 + u_s + u_t$$

- Extract:

$$\hat{y}^{RW2+ICAR}$$

SPDE Matérn

- Construct a triangular mesh from the district centroids.
- Define the Gaussian random field Matérn of SPDE.
- Form the projection matrix A.
- Estimate the model.

$$\log(\lambda_{st})$$

- Extract

$$\hat{y}^{SPDE}$$

Model evaluation and comparation

The estimated of all evaluation criteria are summarized in Table 3.2.

Table 3.2. Comparison of information criteria and predictive performance across models

Model	WAIC	DIC	RMSE	MAE	Spatial R^2
GLM Poisson	5132	4981	5.31	3.82	0.41
CAR (ICAR)	4217	4039	3.47	2.51	0.61
RW2 temporal	4478	4301	3.32	2.40	0.64
SPDE + RW2 + interaction	3547	3481	2.41	1.33	0.82

Model comparison results summarized demonstrate substantial performance gains achieved by the proposed SPDE-INLA framework. Relative to the Poisson GLM, all spatially or temporally structured models exhibit marked improvements, with the SPDE + RW2 + interaction specification yielding the lowest WAIC and DIC values alongside the strongest predictive accuracy. Notably, the reduction in WAIC exceeding 700 points relative to the CAR model highlights the advantage of SPDE in representing spatial dependence over continuous domains.

While CAR models constrain spatial dependence to administrative units, producing blocklike risk patterns aligned with district boundaries, the SPDE formulation operates on a continuous spatial domain, allowing it to capture fine scale local variation consistent with ecological mechanisms of vector dispersal. By leveraging a geometry based triangulated mesh, SPDE effectively generalizes spatial patterns and reproduces smoothly varying risk surfaces.

The SPDE based model achieved the highest spatial predictive performance, with a Spatial $R^2$of 0.82, substantially exceeding that of competing models. Prediction error was reduced by approximately 30% compared with the CAR specification. Moreover, the combined SPDE and RW2 temporal structure produced an RMSE of 2.41, markedly lower than that obtained from the RW2 only model (RMSE = 3.32). These results underscore the complementary contributions of continuous domain spatial modeling and nonparametric temporal smoothing in improving predictive accuracy across both space and time.

Spatial analysis revealed pronounced clustering of dengue risk, particularly in Kambu and Anduonohu districts, characterized by high residential density and accelerated urban expansion. This aligns with ecological indicating that urbanization intensity, housing density, and the abundance of domestic water containers are key drivers of *Aedes aegypti* proliferation. The spatial range estimated from the SPDE model was approximately 11 km, suggesting that dengue risk at a given location remains influenced by surrounding environmental conditions within this radius. Such spatial dependence is consistent with population mobility patterns and the structural configuration of urban space.

The observed spatial correlation likely reflects multiple interacting ecological mechanisms, including surface water flow and drainage networks, land use transitions, and microenvironmental changes induced by urban densification. High risk zones were primarily concentrated in the northern to central parts of Kendari City, whereas several western areas exhibited comparatively

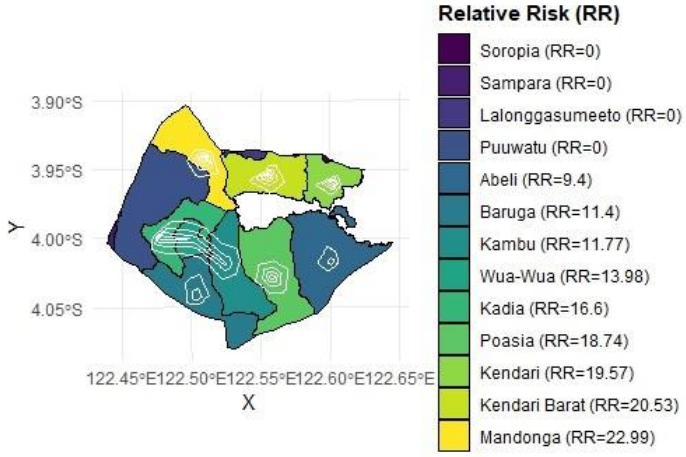

lower risk levels (Figure 3.6).

Figure 3.6. Kendari City Relative risk map of DHF (SPDE)

Dengue control strategies in Kendari City should be implemented in a spatially explicit and targeted manner. Districts exhibiting high risk and steep contour gradients in the urban core, namely Kendari Barat, Kendari, Kadia, Mandonga, Baruga, Kambu, and Wua-Wua districts are recommended as primary priority zones for strengthening vector surveillance. Interventions in these areas should emphasize intensified household-based source reduction and larval source management, including the elimination of water-holding containers, improved solid waste handling, and enhancement of local drainage systems. Within hotspot areas characterized by closed risk contours, control efforts can be further refined at a microspatial scale (approximately 100–300 m) through case triggered selective fogging, complemented by environmental contact tracing to disrupt localized transmission pathways.

In moderate risk zones, interventions should focus on sustained preventive measures, such as community behavior change programs (3M Plus), routine monitoring of larval indices, and the integration of environmental health initiatives with residential planning. Low risk districts may function as buffer zones through the reinforcement of climate informed early warning systems and enhanced passive surveillance capacity, enabling early detection of potential spatial expansion from urban centers. The modeling results also support the implementation of cross sectoral strategies, including the restructuring of densely populated neighborhoods, improvements in sanitation infrastructure, and the management of urban green spaces as part of long-term mitigation efforts.

The continuous risk surface extending beyond administrative boundaries highlights the necessity of inter district coordination, particularly along corridors with pronounced risk gradients. Beyond improving hotspot delineation, the SPDE framework provides a quantitative foundation for adaptive, efficient, and sustainable intervention planning (Table 3.3).

Table 3.3. Risk levels and recommended intervention strategies by district

District	Risk Level	Primary Interventions	Intervention strategy
Kendari Barat	Very High	Hotspot-focused fogging, intensified source reduction (PSN), environmental contact tracing	• Household source reduction (PSN): October–November • Fogging: onset of peak rainfall (December–January) • Weekly monitoring throughout the rainy season
Kendari	Very High	Household-based PSN, weekly larval surveillance	• PSN initiated 1–2 months prior to rainy season • Active surveillance during December–March
Kadia	High	Selective fogging, solid waste management	• Fogging during early case escalation • Routine waste management year-round
Mandonga	High	Community education and community health worker engagement	• Intensive education before rainy season • Strengthening community volunteers during wet months
Baruga	High	Drainage improvement and larval control	• Drainage normalization: September–November • Larviciding: December–February
Kambu	High	Microclimate monitoring	Continuous surveillance
Wua-Wua	High	Early case detection	Active screening at the start of rainy season and during relative risk surges
Abeli	Moderate	Preventive source reduction (PSN)	PSN before rainy season, repeated every two months
Poasia	Moderate	Behavioral change campaigns	October–November campaigns with reinforcement in January–February
Puwatu	Moderate	Larval index monitoring	Assessments during rainy season
Lalodati	Low	Passive surveillance	Quarterly evaluations
Soropia	Low	Buffer-zone monitoring (case migration tracking)	Intensified when neighboring subdistricts report rising cases
Sampara	Low	Climate-informed early warning	Activation of early warning systems during increases in urban core relative risk

4. CONCLUSION AND FUTURE RESEARCH

Study findings reveal pronounced spatio-temporal heterogeneity in DHF risk across Kendari City, with the highest accumulation of risk concentrated in the urban core and along major urban corridors. The Bayesian SPDE–INLA framework consistently outperformed GLM, ICAR, and RW2 models in capturing spatial dependence and continuous risk gradients. Estimated RR

identified Kendari Barat and Kendari districts as the primary transmission epicenters. Kadia, Mandonga, Baruga, Kambu, and Wua-Wua districts were classified as higher risk areas, whereas Abeli, Poasia, and Puuwatu districts exhibited moderate risk levels. In contrast, Lalodati, Soropia, and Sampara districts demonstrated comparatively lower relative risk. Risk contour visualizations revealed distinct spatial clusters aligned with patterns of urban expansion and residential density, highlighting the role of inter district connectivity in shaping dengue transmission dynamics. Integrating RR estimates with intervention timing enabled the formulation of spatially targeted control strategies. In epicentral zones, priority should be given to PSN beginning in October–November, followed by reinforcement during peak rainfall in December–January. High-risk districts require tailored, integrated measures, including selective fogging (Kadia), community education (Mandonga), intensive larval control during December–February (Baruga), microclimate monitoring (Kambu), and active case screening at the onset of the rainy season (Wua-Wua). For moderate risk areas, interventions should emphasize preventive PSN, strengthened behavioral education, and periodic monitoring of larval indices. Low risk districts are best managed through enhanced passive surveillance, development of climate informed early warning systems, and establishment of buffer zones to mitigate spatial spillover from urban centers. Future work will extend the SPDE–INLA framework by integrating mechanistic human vector transmission models, such as SIR–SI or SEI–SEIR structures. In addition, Bayesian predictive control scenario simulations may be employed to evaluate the relative effectiveness of alternative interventions prior to field implementation, with outputs subsequently incorporated into a real time spatial dashboard linked to routine surveillance systems.

FUNDING

This research was supported by the Internal Basic Research Grant of Universitas Halu Oleo under Contract No. 318/UN29.23/PG/2025.

ETHICAL APPROVAL

This manuscript does not report any studies involving human participants conducted by the authors.

DATA AVAILABILITY STATEMENT

The datasets supporting the conclusions of this study are available from the corresponding author upon reasonable request.

CONFLICT OF INTEREST

The authors declare that they have no financial interests or personal relationships that could have influenced, or be perceived to have influenced, the work reported in this paper.

ACKNOWLEDGEMENTS

The authors gratefully acknowledge the Southeast Sulawesi Provincial Health Office and the Environmental Agency for granting access to observational data used in this study. The authors also thank the anonymous reviewers for their constructive comments and valuable suggestions, all of which have been carefully addressed in the revised manuscript and have substantially improved the quality of the final version.

REFERENCES

1. Achee N.L., Gould F., Perkins T.A., Reiner R.C., Morrison A.C., Ritchie S.A., et al., 2015. A Critical Assessment of Vector Control for Dengue Prevention. PLoS Negl Trop Dis 9. https://doi.org/10.1371/journal.pntd.0003655.

2. Alto B.W., Zhang X., Mei H., Nie P., Hu X., Feng J., 2025. Future Climate Predicts Range Shifts and Increased Global Habitat Suitability for 29 Aedes Mosquito Species. https://doi.org/10.3390/insects.
3. Asnita Yani, 2024. The Influence of Environmental Factors on the Development of Dengue Fever. *The International Science of Health Journal* 2:116–23. https://doi.org/10.59680/ishel.v2i4.1569.
4. Belmont J.., Martino S., Illian J., Rue H.,2-24. Spatio-temporal occupancy models with INLA. *Methods Ecol Evol*, 15, 2087–100. https://doi.org/10.1111/2041-210X.14422.
5. Clarotto L., Allard D., Romary T., Desassis N., 2024. The SPDE approach for spatio-temporal datasets with advection and diffusion. *Spat Stat,* 62. https://doi.org/10.1016/j.spasta.2024.100847.
6. Cortés R.R., Thanjangreed W., Chertenko T., 2025. Relationship Between Environmental Sanitation and Dengue Hemorrhagic Fever Incidents. *Journal of Health Innovation and Environmental Education*, 2,43–51. https://doi.org/10.37251/jhiee.v2i1.1736.
7. Feng F., Ma Y., Zhao Y., Liu Z., Zhang R., Wan Z., 2025. Assessment of Global Dengue Transmission Risk Under Future Climate Scenarios. *Earths Future*,13. https://doi.org/10.1029/2025EF006154.
8. Gubler D.J., 2011. Dengue, Urbanization and globalization: The unholy trinity of the 21 st century. *Trop Med Health*, 39, 3–11. https://doi.org/10.2149/tmh.2011-S05.
9. Ipa M., Hermawan A., Yunarko R., Ramadhani T., Hidajat M.C., Hendarwan H., et al., 2026. Urban-rural disparities in self-reported dengue infection: A comprehensive analysis of the 2023 Indonesian health survey. *Glob Transit*, 8, 10–21. https://doi.org/10.1016/j.glt.2025.08.003.
10. Jaya I.G.N.M., Folmer H., 2024. High-Resolution Spatiotemporal Forecasting with Missing Observations Including an Application to Daily Particulate Matter 2.5 Concentrations in Jakarta Province, Indonesia. *Mathematics*, 12. https://doi.org/10.3390/math12182899.
11. Lindgren F., Rue H., Lindström J., 2011. An explicit link between Gaussian fields and Gaussian Markov random fields. *The stochastic partial differential equation approach*. vol. 73.
12. Lindgren F., 2015. Bayesian Spatial Modelling with R-INLA. vol. 63.
13. Liu-Helmersson J., Rocklöv J., Sewe M., Brännström Å., 2019. Climate change may enable Aedes aegypti infestation in major European cities by 2100. *Environ Res,* 172:693–9. https://doi.org/10.1016/j.envres.2019.02.026.
14. Mamenun, Koesmaryono Y., Sopaheluwakan A., Hidayati R., Dasanto B.D., Aryati R., 2024. Spatiotemporal Characterization of Dengue Incidence and Its Correlation to Climate Parameters in Indonesia. *Insects*, 15. https://doi.org/10.3390/insects15050366.
15. Muhamad F.T., Azizah R., 2023. The Impact of Environmental and Behavioral Factors on the Incidence of Dengue Hemorrhagic Fever in Indonesia: Meta-analysis. *Poltekita : Jurnal Ilmu Kesehatan*, 17:762–70. https://doi.org/10.33860/jik.v17i3.3133.
16. Mukhsar, Tenriawaru A., Wibawa G.N.A., Abapihi B., Ahmad S.W., Sudayasa I.P., 2025. Bayesian Stochastic INLA Application to the SIR-SI Model for Investigating Dengue Transmission Dynamics. *Intelligent Automation and Soft Computing*, 40:177–93. https://doi.org/10.32604/iasc.2025.058884.

17. Mukhsar, Wibawa G.N.A., Tenriawaru A., Usman I., Firihu M.Z., Variani V.I., et al., 2023. Stochastic Bayesian Runge-Kutta method for dengue dynamic mapping. *MethodsX*, 10. https://doi.org/10.1016/j.mex.2022.101979.
18. Nakase T., Giovanetti M., Obolski U., Lourenço J., 2023. Global transmission suitability maps for dengue virus transmitted by Aedes aegypti from 1981 to 2019. *Sci Data*, 10. https://doi.org/10.1038/s41597-023-02170-7.
19. Rubino C., Di Maria C., Abbruzzo A., Bono G., Garofalo G., Milisenda G., et al., 2025. Derivative-based spatial mediation with INLA-SPDE. *Spat Stat*, 66. https://doi.org/10.1016/j.spasta.2025.100885.
20. Rulli, M.C., D'Odorico P., Galli N., John R.S., Muylaert R.L., Santini M., et al., 2025. Land Use Change and Infectious Disease Emergence. *Reviews of Geophysics,* 63. https://doi.org/10.1029/2022RG000785.
21. Salim M.F., Satoto T.B.T., Danardono, 2025. Understanding local determinants of dengue: a geographically weighted panel regression approach in Yogyakarta, Indonesia. *Trop Med Health* , 53. https://doi.org/10.1186/s41182-025-00734-4.
22. Saldaña F., Stollenwerk N., Van Dierdonck J.B., Aguiar M., 2024. Modeling spillover dynamics: understanding emerging pathogens of public health concern. *Sci Rep*, 14. https://doi.org/10.1038/s41598-024-60661-y.
23. Sani A., Abapihi B., Mukhsar, Tosepu R., Usman I., Rahman G.A., 2023. Bayesian temporal, spatial and spatio-temporal models of dengue in a small area with INLA. *International Journal of Modelling and Simulation*, 43:939–51. https://doi.org/10.1080/02286203.2022.2139108.
24. Sureshkumar S., Shekhar S., 2025. Impact of urban heat island effect on dengue incidence: a remote sensing approach using thermal and high-resolution optical imagery. *BMC Public Health*, 25. https://doi.org/10.1186/s12889-025-23763-4.